iJRASET
International Journal For Research in Applied Science and Engineering Technology

INTERNATIONAL JOURNAL FOR RESEARCH

IN APPLIED SCIENCE & ENGINEERING TECHNOLOGY

Volume: 8 **Issue:** V **Month of publication:** May 2020

DOI: http://doi.org/10.22214/ijraset.2020.5346

www.ijraset.com

Call: 08813907089 | E-mail ID: ijraset@gmail.com

International Journal for Research in Applied Science & Engineering Technology (IJRASET)
ISSN: 2321-9653; IC Value: 45.98; SJ Impact Factor: 7.429
Volume 8 Issue V May 2020- Available at www.ijraset.com

Epidermal Antenna for UHF-RFID Application

Ankita Choudhury[1], Shambavi K[2]
[1, 2]*Department of Communication, School of Electronics Engineering, VIT, Vellore, Tamil Nadu*

***Abstract:** In this paper, an epidermal antenna operating at UHF range of 860-960 MHz is presented. The proposed design is a slot antenna with total patch size of 66.10 x 45.95 mm^2. The substrate material considered in this design is cotton textile pertaining to the basic requirement of the epidermal antenna to be flexible, comfortable on skin, easily available and inexpensiveness. Use of tapered terminals for proper impedance matching with the RFID chip and the effect of its width optimization on the performance parameters are discussed. The proposed design is simulated on different body tissue layers to test its behaviour on different dielectric properties. In addition, effect of bending with different radius is also studied to determine the response of antenna for conformism.*
***Keywords:** UHF, RFID, epidermal antenna, slot antenna, human tissues.*

I. INTRODUCTION

Wearable technology in the recent years has gained popularity worldwide and has encouraged researchers to initiate studies in field of material science, electromagnetics, electronics and communication and so on. Wireless body area network (WBAN) has attracted many such applications be it a body worn device [1]–[4] or implanted [5]–[8]. The major challenges faced by the antennas in this technology are high dielectric losses offered by the antenna platform which is a human body in this case. Many wearable antennas have successfully overcome the issue with the use of multi-layer antennas which significantly increased the gain and also improved the Front-to-back ratio.

On the contrary, epidermal antenna being a specific area of wearable application doesn't encourage the use of multi layer for its requirement to be in contact with the skin and maximum allowable thickness as 1mm. In such cases, use of single layer antenna is observed in many research works mainly dipole antenna [9]–[11], loop antenna [12]–[14] and slot antenna [15], [16] . It can be observed in all these works that the gains obtained with the use of single layer structures are negative. The effect of human body tissues on the gain of the antenna is discussed in [17] .

The integration of wearable antenna with RFID to produce wearable tag has further opened discussions about the matching techniques [18] in order to match the antenna impedance with chip impedance. The most popular techniques are T-matching techniques, nested slot and inductively coupled loop. For the use of such devices in compact spaces the antennas are required to be miniaturized in a way that supports its application.

The behaviour of the epidermal antenna is majorly governed by the human body tissues and the materials used to make them pertaining to their requirement of flexibility, stretch-ability, conformism and breathablilty. In case of more intimate application the materials are also required to be bio-compatible in nature. The most common materials with the aforementioned properties are textile materials [19] and silicon based polymers [20].

II. ANTENNA DESIGN

The design of the tag antenna is carried out by considering the various factors like the dielectric constant of all the tissues and the operating frequency of 900 MHz. Hence, calculations are carried out accordingly. All the performance parameters obtained were designed in association with tag IC chip (considering Impinj Monza 5 IC [21] with chip impedance Z_{IC} = 33- j *113 ohm and P_{IC} = -17.8dBm) for the frequency range of 860-960MHz which is considered to be worldwide range for RFID applications.The layout of the tag antenna designed in this project is a single-layer hexagonal shaped slot antenna.The dielectric material considered for the design is cotton textile with thickness of 0.05mm and permittivity of 1.6 F/m and loss tangent of 0.04.

A. Determining the effective Permittivity of Tissues

Designing an antenna for epidermal application requires the study of dielectric properties of the bio-tissue layers (human body). To initiate any design it is important to determine the wavelength for a particular frequency which is affected by the relative permittivity of the tissues. To start with, a stratified tissue model 200 x 200 x 168 mm3 was considered which constitutes four layers namely (in order from top to bottom) skin and fat, muscle, bone and viscera. The thickness and the electrical properties of the layers are mentioned in the TABLE I [22]

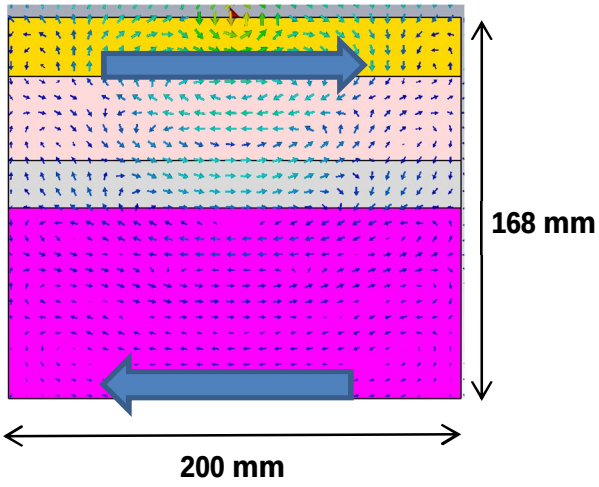

Fig. 1 Representational layered model of human tissue

Consider the direction of E-field as shown by the arrow in Fig. 1. If two sides of the model is considered to be plates of a capacitor parallel to each other and the distance (d) between them is 200mm, the area (A) of the two sides as (168mm x 200mm) (the area of sides of each layer depends on thickness of individual tissues); then the equivalent relative permittivity can be found following equations [23]:

$$C_{tissue} = \frac{\varepsilon_0 \varepsilon_r A}{d} \tag{1}$$

$$C_{phantom} = C_{skin+fat} + C_{muscle} + C_{bone} + C_{organs} \tag{2}$$

$$\varepsilon_{phantom} = \frac{C_{phantom}}{C_0} \tag{3}$$

TABLE I
Physical And Geometrical Parameters Of The Layered Anatomical Model At 900 Mhz

Layers	Relative Permittivity (ε_r)	Conductivity (S/m)	Thickness (mm)
Skin + fat	14	0.25	26
Muscle	55.032	0.94	37
Bone	12.45	0.14	21
Internal organ	52.1	0.91	84

Following the equations the permittivity of the layered model is found to be $\varepsilon_{phantom}$ = 43 F/m. Also, the conductivity of the model is assumed to be 0.9 S/m [24]. Now, with the obtained permittivity of the phantom along with that of air, effective permittivity (ε_{eff}) as sensed by the antennas when installed on the model, is given by (4)

$$\varepsilon_{eff} = \frac{\varepsilon_{phantom} + 1}{2} \tag{4}$$

Hence, effective wavelength (λ_{eff}) is given by (6),

$$\lambda_0 = \frac{c}{f} \tag{5}$$

$$\lambda_{eff} = \frac{\lambda_0}{\sqrt{\varepsilon_{eff}}} \tag{6}$$

B. Antenna Design Evolution Stages

The antenna designed for 900 MHz was initially developed in its first stage with the dimension as theoretically calculated in the previous section. Consequently, changes were made by optimization of the structure using CST Studio SUITE 2019 to obtain desirable performance characteristic of the antenna. All stages were simulated on the layered tissue model and corresponding outputs are presented. The very first aim to make such antenna perform well is the impedance matching of the tag antenna ($Z_A=R_A+ j*X_A$) with the tag chip ($Z_{IC}=R_{IC}+ j*X_{IC}$) as mentioned in equation (7).

$$Z_A = Z_{IC}^* \tag{7}$$

that is,

$$R_A = R_{IC} \tag{8}$$

$$X_A = -X_{IC} \tag{9}$$

1) Stage 1: A simple hexagonal structure with slots was first designed with the obtained wavelength for the radiating element. Fig. 2 shows the structure of stage 1. The realized gain presented in Fig. 4 can corroborate to the lossy nature of human tissues and hence the negative gain. The stage 1 antenna clearly fails to perform in terms of impedance matching which is evident from the S11 parameter shown in Fig. 3. Hence further changes were necessary to obtain a desirable outcome.

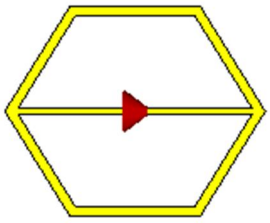

Fig. 2 Stage 1 antenna structure

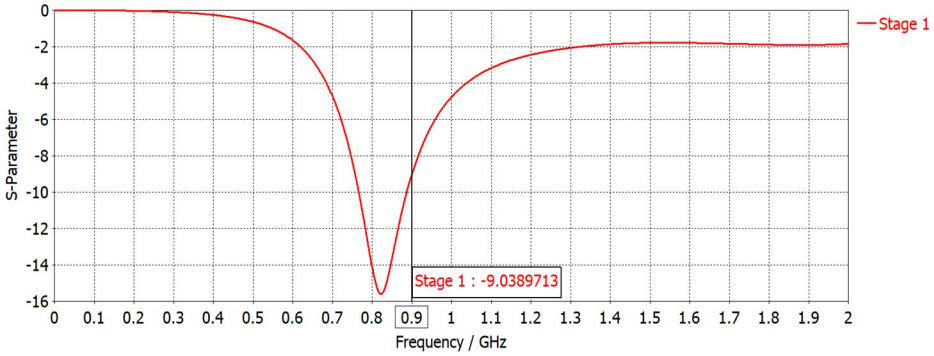

Fig. 3 Stage 1: S11 parameter

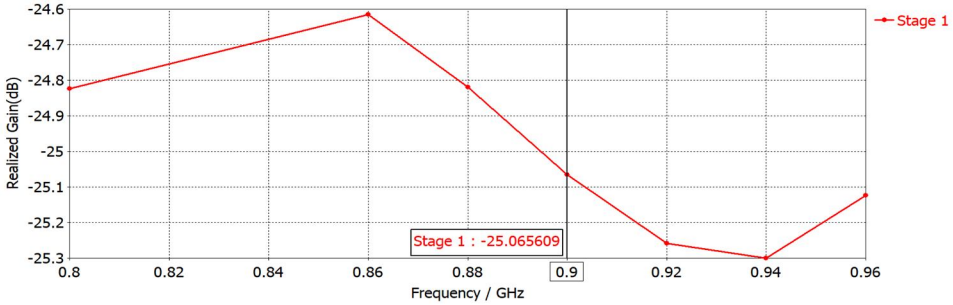

Fig. 4 Stage 1: Realized Gain

2) *Stage 2:* The terminals were tapered (Fig. 5) and its width was optimized to obtain a proper impedance matching with the chip in this stage. The effect of tapering was not only observed in the impedance matching (Fig. 6) but also it improved the gain (Fig. 10) by a margin of 2dB, though it was not still satisfactory.

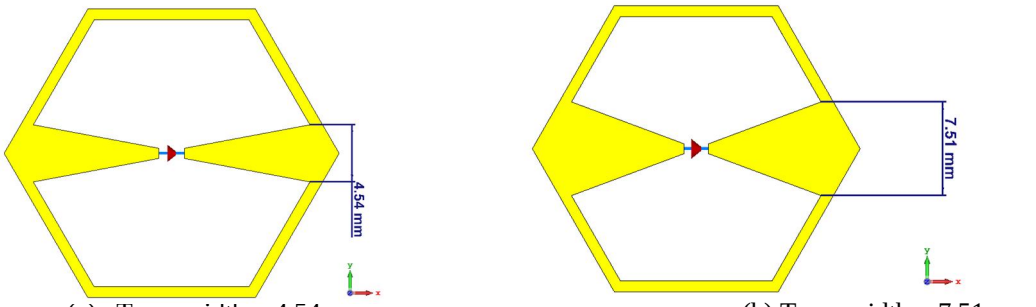

(a) Taper width = 4.54 mm (b) Taper width = 7.51 mm

Fig. 5 Stage 2: Taper width optimization

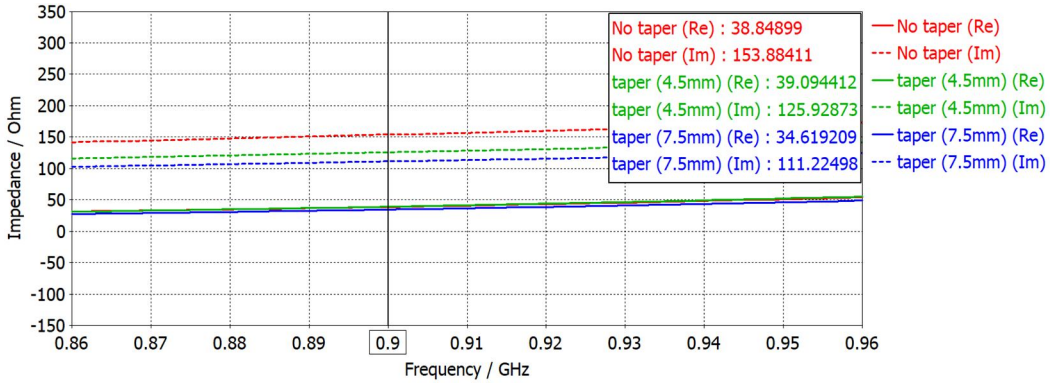

Fig 6 Stage 2: Impedance upon taper width optimization

The stage 2 antenna was not only tested for tapering width but also its trace width was optimized. It has been observed that the trace width has insignificant influence on the gain of the antenna; however it did have effect on the impedance of the antenna. The effect on simulated gain and impedance of the antenna upon trace width optimization can be observed from the following figures respectively:

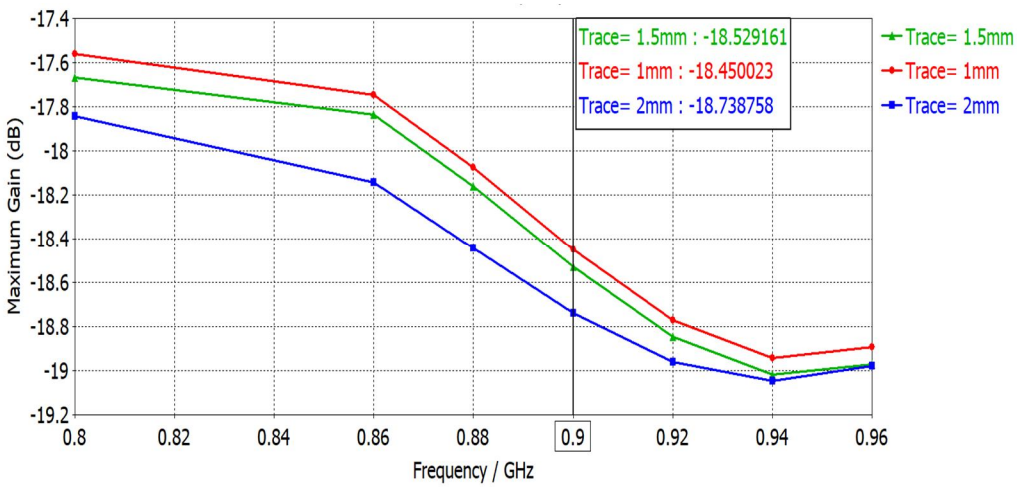

Fig. 7 Stage 2: Maximum Gain upon trace width optimization

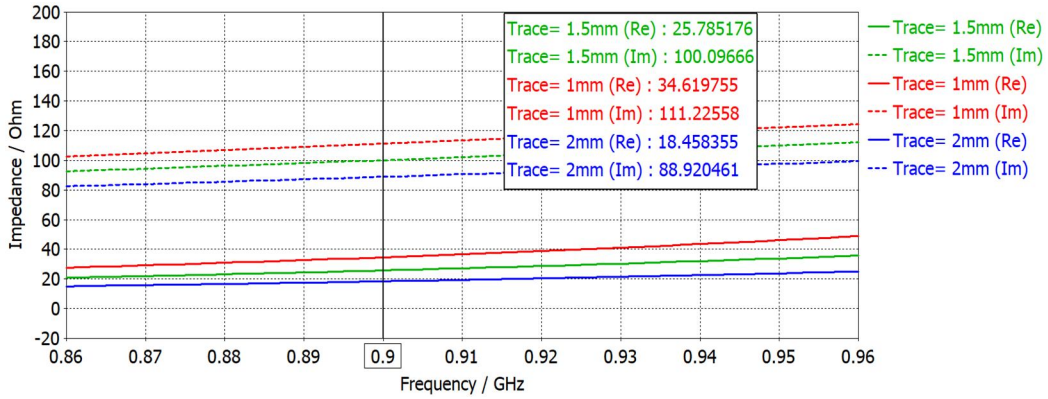

Fig. 8 Stage 2: Impedance upon trace width optimization

With trace width of 1mm and taper width of 7.5mm the obtained impedance can be observed as 34.6+j*111.2 ohm which can be considered to be an effective match between the antenna and the RFID chip and with a simulated maximum gain of -18.4 dB. The S11 parameter of both the antenna structures is shown in Fig. 9 and the realized gain of the stage 2 antenna is shown in Fig. 10.Though the impedance achieved by stage 2 was satisfactory but the gain obtained was not impressive.

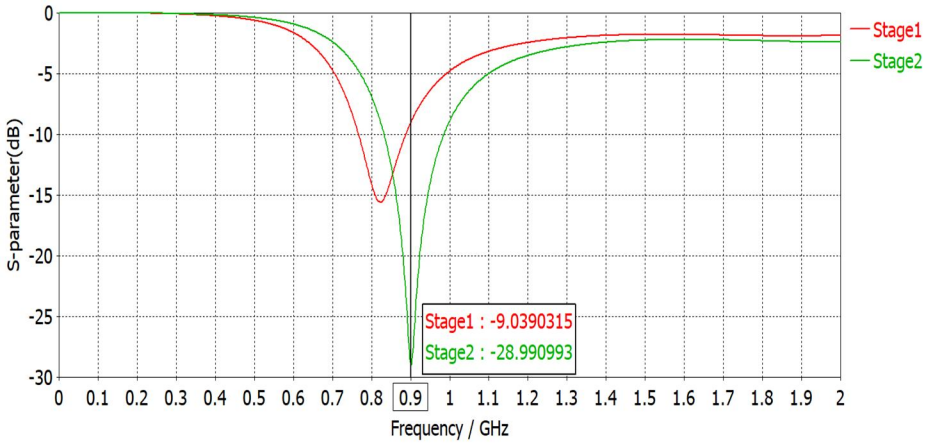

Fig. 9 S11 parameter comparison Stage 1 and 2

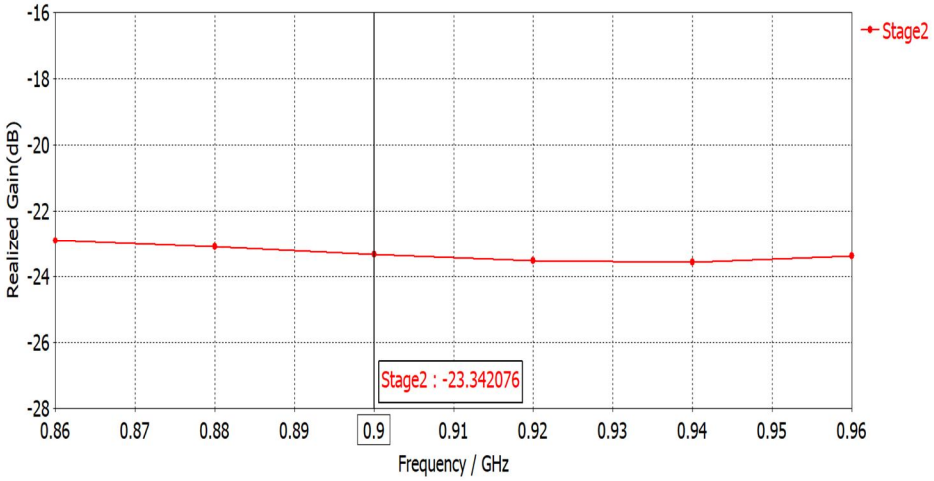

Fig. 10 Stage 2: Realized Gain

3) Stage 3: Though the resonance and the impedance matching were obtained in stage 2 of the process, there was scope for improvement for the gain which is discussed in stage 3 of antenna. Four patches of similar shape (hexagonal) as that of the antenna mentioned in earlier stages were added to stage 2 antenna with the purpose of improving the gain.The overall size of the radiating element (Fig. 11) after addition of the patches was 6.6 cm x 4.59 cm, a size which can be considered very optimal to be used as on skin antenna.

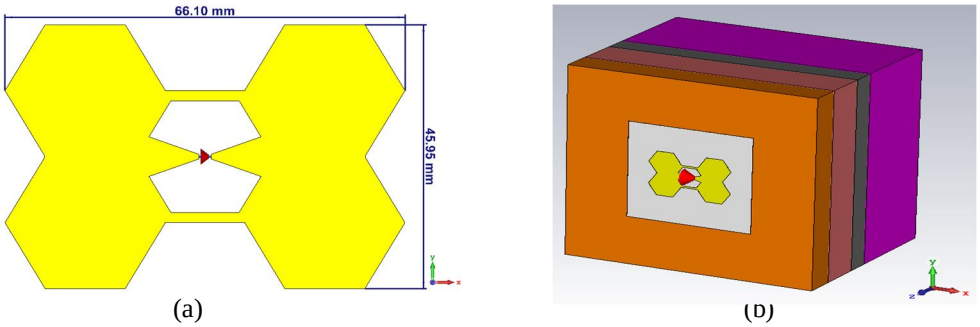

(a) (b)

Fig. 11 Stage 3 antenna structures

Significant changes can be observed in stage 3 once the patches were added which can be confirmed with the comparison made between the realized gain (Fig. 12), Impedance (Fig. 13) and S11 parameter (Fig. 14) of stage 2 and stage 3. The impedance matching can be seen to improve further to 33.5+j*111.8 ohm and significant shift in the realized gain from -23.34 dB (stage 2) to -15.74dB (stage 3) that is by the margin of 8dB. The radiation pattern of the antenna when simulated over the layered tissue model shows that the direction of the maximum radiation is on the frontal direction (Fig.15), i.e. perpendicular to the model, which is desirable for this application.

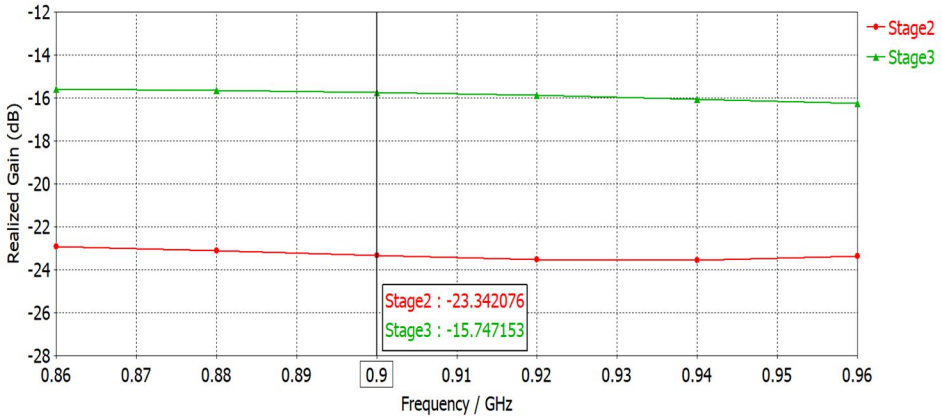

Fig. 12 Realized gain comparison between stage 2 and 3

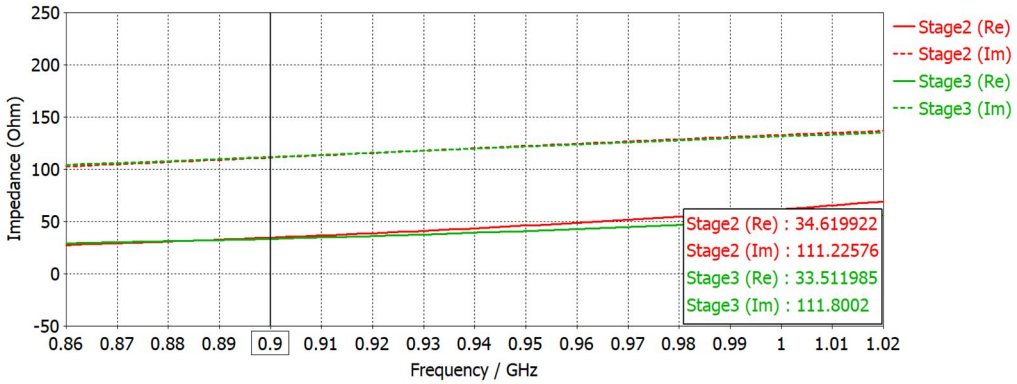

Fig. 13 Impedance comparison between stage 2 and 3

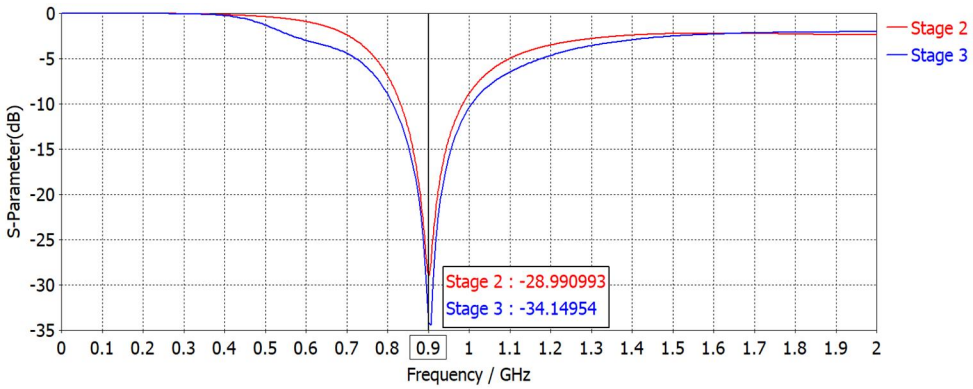

Fig. 14 S11 comparison between stage 2 and 3

Using the layered model has given a perspective on how an epidermal antenna behaves on bio-tissue layers of human body which is the main reason of the obtained negative gain. Also, the nature of antenna structure being a 'single layer' one the improvement in the gain using another layer (EBG or ground plane) is out of scope.

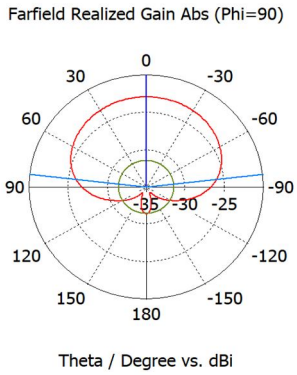

Fig. 15 Stage 3: Radiation pattern

III. SIMULATION RESULTS OVER DIFFERENT BODY REGIONS

The composition of human body is not homogeneous all through. The body we see from the outside which appears symmetrical from a distance is not the same on the inside. The skin being the outermost layer is the largest organ of the body stretching from 'tip to toe' is also not uniform all over with the presence of pores, hair, curves and bumps on it. Tissues in different regions of the body are versatile and also the organs within each region have different dielectric properties. The permittivity and the loss tangent of certain organs and tissues used in this paper are mentioned in the graph given in TABLE II. The stage 3 design that was simulated over the layered model was also tested on four layered models of different body regions with their corresponding properties.

TABLE II
Reference Tissue Layer Thickness Of Different Body Regions

Tissues	Limb (mm)	Abdomen (mm)	Thorax (mm)	Forehead (mm)
Skin	2.6	2.6	2	2
Fat	8	11	-	2
Muscle	24	20	4	-
Bone	12	-	10	8
Dura	-	-	-	1.5
CSF	-	-	-	2
Viscera	Bone	Intestine	Lungs	Brain

TABLE III
Relative Permittivity And Loss Tangent Of Tissues [22]

Tissues	Relative permittivity (F/m)	Loss Tangent
Bone	12.45	0.23
Brain	48.30	0.29
Cerebrospinal fluid (CSF)	68.64	0.70
Dura	44.40	0.43
Fat	5.46	0.19
Viscera	52.09	0.35
Intestine	59.49	0.73
Lungs	36.70	0.33
Muscle	55.03	0.34
Skin	41.40	0.39

Four layered tissue model of different regions namely the abdomen, thorax, limb and forehead as shown in Fig. 16 was taken into consideration owing to the fact that the nature of tissue composition and different organs underneath provided versatile platform for the antenna. Not only the dielectric properties but also the thickness of the layers was considered (TABLE III) to make their respective models.

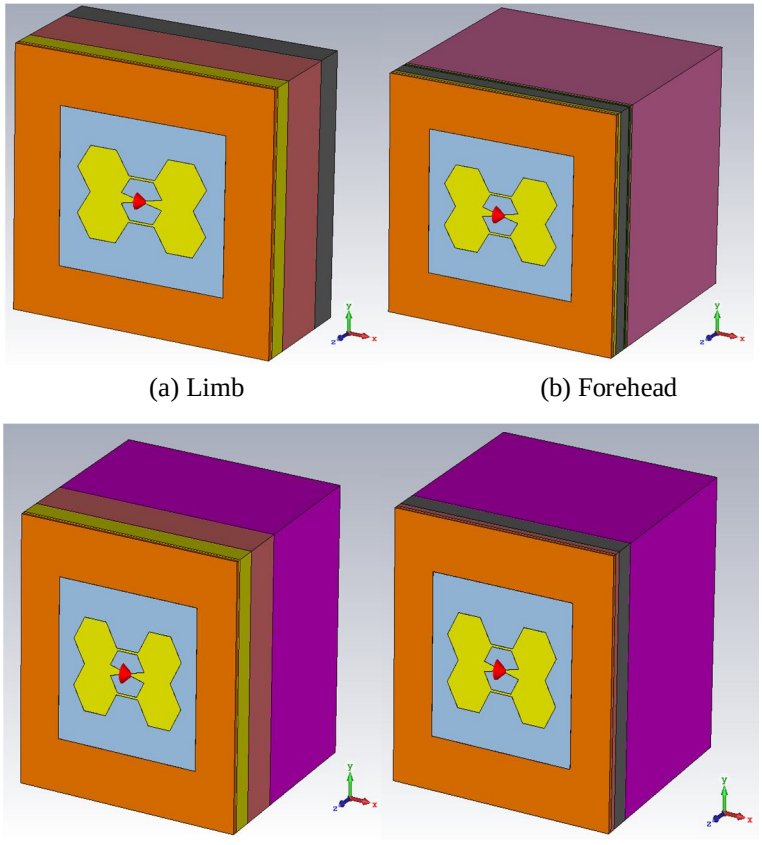

(a) Limb (b) Forehead

(c) Abdomen (d) Thorax

Fig. 16: Model of different body districts

The body regions considered can be classified based on that that limb and abdomen are high in water content while the thorax and skull sees significant presence of bone. Fig. 17 shows the realized gain of the antenna on the body regions mentioned above. It can be observed that there is a difference of 2-3dB between the gain of the aforementioned two classifications.

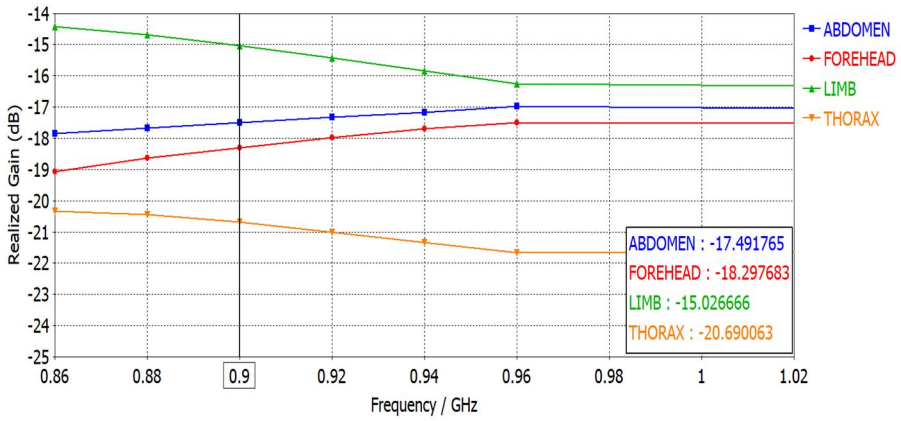

Fig. 17 Realized gain of antenna placed over different body regions

Of the two classifications, it can be seen that the one with more water content i.e. the limb and the abdomen have good performance as compared to the other class i.e. the forehead and the thorax region. Fig. 18 shows the antenna impedance of the antenna. All the performance parameters mentioned in the section shows the sensitivity of the tag to the specific parts of the body. The power transmission coefficient (τ) listed in TABLE IV for different body regions was theoretically calculated for various body regions used in this simulation using the equation given below (10).

$$\tau = \frac{4R_A R_{IC}}{\left|Z_A + Z_{IC}\right|^2} < 1 \qquad (10)$$

where, R_A = Resistance of the antenna
R_{IC}=Resistance of RFID chip
Z_A=Impedance of antenna
Z_{IC}=Impedance of RFID chip

TABLE IV
Power Transmission Coefficient Of Antenna Over Different Body Regions

Body Districts	Power Transmission Coefficient (τ)
Abdomen	0.88
Forehead	0.89
Limb	0.9
Thorax	0.95

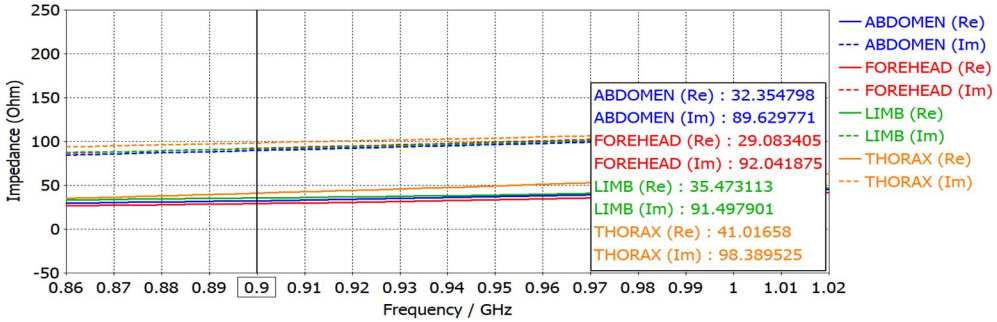

Fig. 18 Impedance of antenna placed over different body regions

IV. SIMULATION RESULTS OVER DIFFERENT BODY MASS

In order to test the effect of bending of the epidermal antenna on curved surface, a finite cylindrical model (as shown in Fig. 19 (b)) with different radius representing the characteristics of arm is considered which is constituted of different layers like the skin, fat, muscle and the cortical bone with their respective values of permittivity (TABLE III) and is simulated for 900 MHz. The cross section of cylindrical layer model of arm is shown in Fig 19 (a). .Three different models of varying dimension of the arm tissues were considered which are stated in the TABLE IV.

TABLE IV
Radius Of Three Cylindrical Phantom Model

Model	R_{skin} (mm)	R_{fat} (mm)	R_{muscle} (mm)	R_{bone} (mm)
Small (A)	38	35	27	15
Medium (B)	48	45	37	15
Large (C)	64	61	53	15

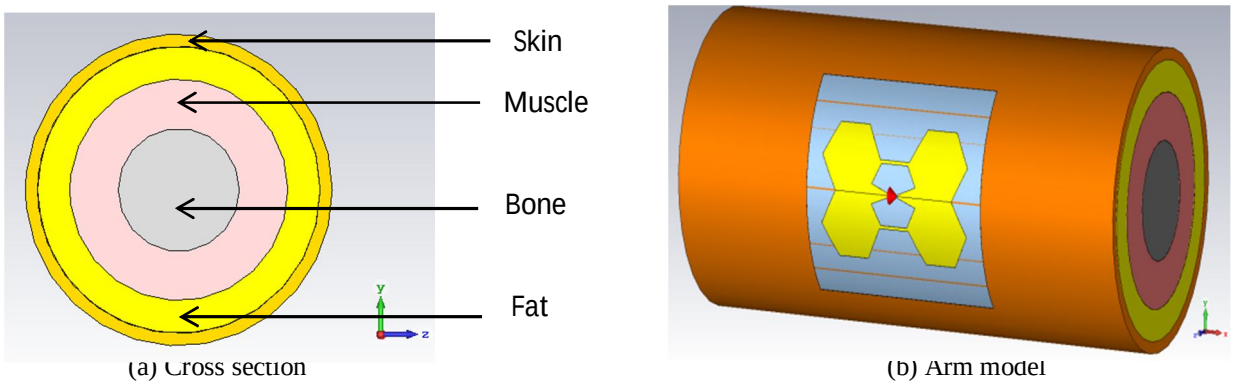

(a) Cross section (b) Arm model

Fig. 19 Cylindrical Phantom model

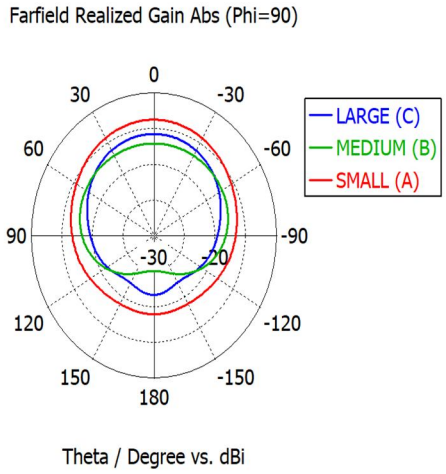

Fig. 20: Radiation pattern of antenna on three cylindrical phantom model

The impedance and realized gain obtained by bending the antenna to three different models are shown in Fig. 21 and Fig. 22 respectively. Power transmission coefficient (τ), FBR and efficiency of three models are listed in TABLE V. As expected model (A) with the smallest radius has the best gain and FBR of all the three models and is favorable to establish the RFID link. The gain radiation pattern (Fig. 20) shows that the radiation takes place perpendicular to the tag in all the three cases which is desirable for the application.

TABLE V
Performance Parameters

Model	Power transmission coefficient (τ)	FBR	Efficiency
Small (A)	0.94	5.9	4%
Medium (B)	0.93	2.3	5%
Large (C)	0.92	5.2	3%

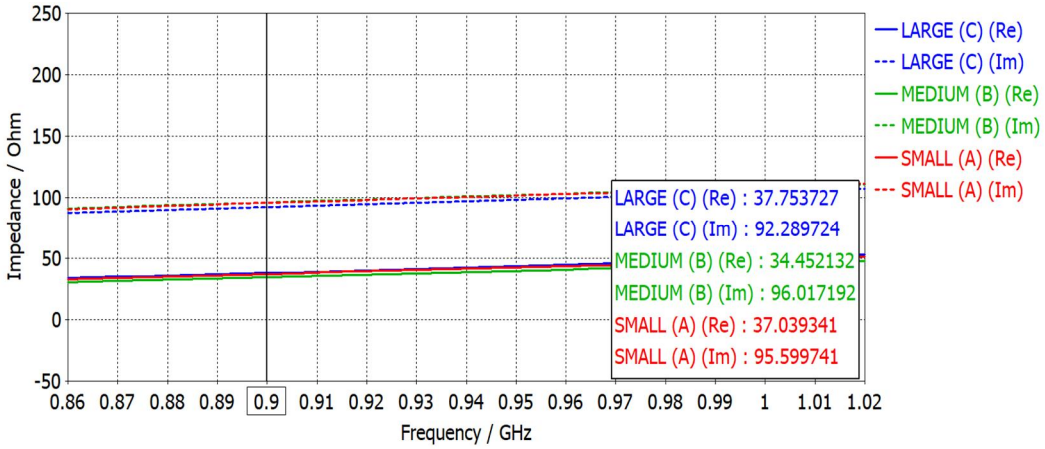

Fig. 21 Impedance of antenna on three cylindrical phantom model

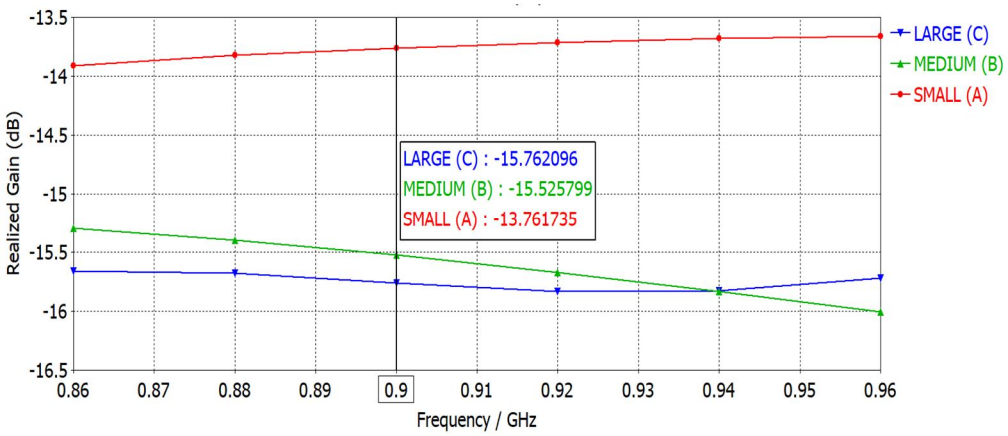

Fig. 22 Realized gain of antenna on three cylindrical phantom model

V. CONCLUSION

It was evident that the antenna performance parameters were severely affected by the permittivity and losses of the antenna platform i.e. bio-tissue layers. The use of textile material (cotton as substrate material) encouraged to design this antenna was chosen pertaining to its flexibility, conformism, availability, inexpensiveness and its ability to allow the skin to breathe which all the required characteristics to design epidermal antenna. The design of the proposed antenna was motivated by the single layer structure of slot antenna. The addition of hexagonal patches to stage 2 design has resulted in significant increase in the gain and the use of tapered terminal has resulted in a good match of the antenna impedance with the chip impedance. The effect of trace width optimization is not significant in case of gain whereas notable effects were observed in the impedance of the antenna. Simulations demonstrated that the proposed antenna on cotton textile substrate provide a realized gain of -15dB to -21dB when placed on different body regions whereas when tested for conformism on different bending radius the obtained realized gain ranges from -13.7dB to -15.7dB. The maximum radiation occurred at the frontal direction i.e. perpendicular to where it is placed over the body.

REFERENCES

[1] M. Akbari, L. Sydanheimo, Y. Rahmat-Sami, J. Virkki, and L. Ukkonen, "Implementation and performance evaluation of graphene-based passive UHF RFID textile tags," 2016 URSI Int. Symp. Electromagn. Theory, EMTS 2016, pp. 447–449, 2016, doi: 10.1109/URSI-EMTS.2016.7571422.
[2] C. Occhiuzzi and G. Marrocco, "The RFID technology for neurosciences: Feasibility of Limbs' monitoring in sleep diseases," IEEE Trans. Inf. Technol. Biomed., vol. 14, no. 1, pp. 37–43, 2010, doi: 10.1109/TITB.2009.2028081.
[3] M. C. Tsai, C. W. Chiu, H. C. Wang, and T. F. Wu, "Inductivelycoupled loop antenna design for UHF RFID on-body applications," Prog. Electromagn. Res., vol. 143, no. November, pp. 315–330, 2013, doi: 10.2528/PIER13080707.
[4] M. A. Ziai and J. C. Batchelor, "Temporary on-skin passive UHF RFID transfer tag," IEEE Trans. Antennas Propag., vol. 59, no. 10, pp. 3565–3571, 2011, doi: 10.1109/TAP.2011.2163789.
[5] H. Ishihata et al., "A radio frequency identification implanted in a tooth can communicate with the outside world," IEEE Trans. Inf. Technol. Biomed., vol. 11, no. 6, pp. 683–685, 2007, doi: 10.1109/TITB.2007.891926.
[6] T. Ativanichayaphong et al., "Development of an implanted RFID impedance sensor for detecting gastroesophageal reflux," 2007 IEEE Int. Conf. RFID, IEEE RFID 2007, pp. 127–133, 2007, doi: 10.1109/RFID.2007.346160.
[7] C. Occhiuzzi, G. Contri, and G. Marrocco, "Design of implanted RFID tags for passive sensing of human body: The STENTag," IEEE Trans. Antennas Propag., vol. 60, no. 7, pp. 3146–3154, 2012, doi: 10.1109/TAP.2012.2198189.
[8] R. Lodato, V. Lopresto, R. Pinto, and G. Marrocco, "Numerical and experimental characterization of through-the-body UHF-RFID links for passive tags implanted into human limbs," IEEE Trans. Antennas Propag., vol. 62, no. 10, pp. 5298–5306, 2014, doi: 10.1109/TAP.2014.2345586.
[9] A. Kiourti and J. L. Volakis, "Stretchable and flexible E-fiber wire antennas embedded in polymer," IEEE Antennas Wirel. Propag. Lett., vol. 13, pp. 1381–1384, 2014, doi: 10.1109/LAWP.2014.2339636.
[10] S. Shao, A. Kiourti, R. J. Burkholder, and J. L. Volakis, "Broadband textile-based passive UHF RFID tag antenna for elastic material," IEEE Antennas Wirel. Propag. Lett., vol. 14, no. c, pp. 1385–1388, 2015, doi: 10.1109/LAWP.2015.2407879.
[11] K. Koski, L. Sydänheimo, Y. Rahmat-Samii, and L. Ukkonen, "Fundamental characteristics of electro-textiles in wearable UHF RFID patch antennas for body-centric sensing systems," IEEE Trans. Antennas Propag., vol. 62, no. 12, pp. 6454–6462, 2014, doi: 10.1109/TAP.2014.2364071.
[12] S. Amendola, G. Bovesecchi, A. Palombi, P. Coppa, and G. Marrocco, "Design, Calibration and Experimentation of an Epidermal RFID Sensor for Remote Temperature Monitoring," IEEE Sens. J., vol. 16, no. 19, pp. 7250–7257, 2016, doi: 10.1109/JSEN.2016.2594582.
[13] S. Milici, S. Amendola, A. Bianco, and G. Marrocco, "Epidermal RFID passive sensor for body temperature measurements," 2014 IEEE RFID Technol. Appl. Conf. RFID-TA 2014, pp. 140–144, 2014, doi: 10.1109/RFID-TA.2014.6934216.
[14] S. Amendola, S. Milici, and G. Marrocco, "Performance of Epidermal RFID Dual-loop Tag and On-Skin Retuning," IEEE Trans. Antennas Propag., vol. 63, no. 8, pp. 3672–3680, 2015, doi: 10.1109/TAP.2015.2441211.
[15] Y. Zhou, "A novel slot antenna for UHF RFID tag," in IET Conference Publications, 2010, vol. 2010, no. 569 CP, pp. 254–257, doi: 10.1049/cp.2010.0664.
[16] C. Y. D. Sim, W. S. Liao, and J. R. Liou, "Broadband Slot Antenna Design for On-Body UHF RFID Applications (Invited)," Proc. 2018 IEEE 7th Asia-Pacific Conf. Antennas Propagation, APCAP 2018, pp. 526–527, 2018, doi: 10.1109/APCAP.2018.8538053.
[17] H. Abu Damis, "Epidermal Loop Antennas," 2017.
[18] G. Marrocco, "The art of UHF RFID antenna design: Impedance-matching and size-reduction techniques," IEEE Antennas and Propagation Magazine, vol. 50, no. 1, pp. 66–79, 2008.
[19] R. Salvado, C. Loss, Gon, and P. Pinho, "Textile materials for the design of wearable antennas: A survey," Sensors (Switzerland), vol. 12, no. 11, pp. 15841–15857, 2012, doi: 10.3390/s121115841.
[20] H. A. Damis, N. Khalid, R. Mirzavand, H. J. Chung, and P. Mousavi, "Investigation of Epidermal Loop Antennas for Biotelemetry IoT Applications," IEEE Access, vol. 6, pp. 15806–15815, 2018, doi: 10.1109/ACCESS.2018.2814005.
[21] A. Singh and P. J. Kaur, "Proceeding of the Second International Conference on Microelectronics, Computing & Communication Systems (MCCS 2017)," 2019, vol. 476, no. Mccs 2017, pp. 689–699, doi: 10.1007/978-981-10-8234-4.
[22] "Dielectric Properties of Body Tissues: HTML clients." http://niremf.ifac.cnr.it/tissprop/htmlclie/htmlclie.php (accessed May 22, 2020).
[23] H. A. Damis, N. Khalid, R. Mirzavand, H. J. Chung, and P. Mousavi, "Investigation of Epidermal Loop Antennas for Biotelemetry IoT Applications," IEEE Access, vol. 6, pp. 15806–15815, Mar. 2018, doi: 10.1109/ACCESS.2018.2814005.
[24] S. Amendola and G. Marrocco, "Optimal Performance of Epidermal Antennas for UHF Radio Frequency Identification and Sensing," IEEE Trans. Antennas Propag., vol. 65, no. 2, pp. 473–481, 2017, doi: 10.1109/TAP.2016.2639829.

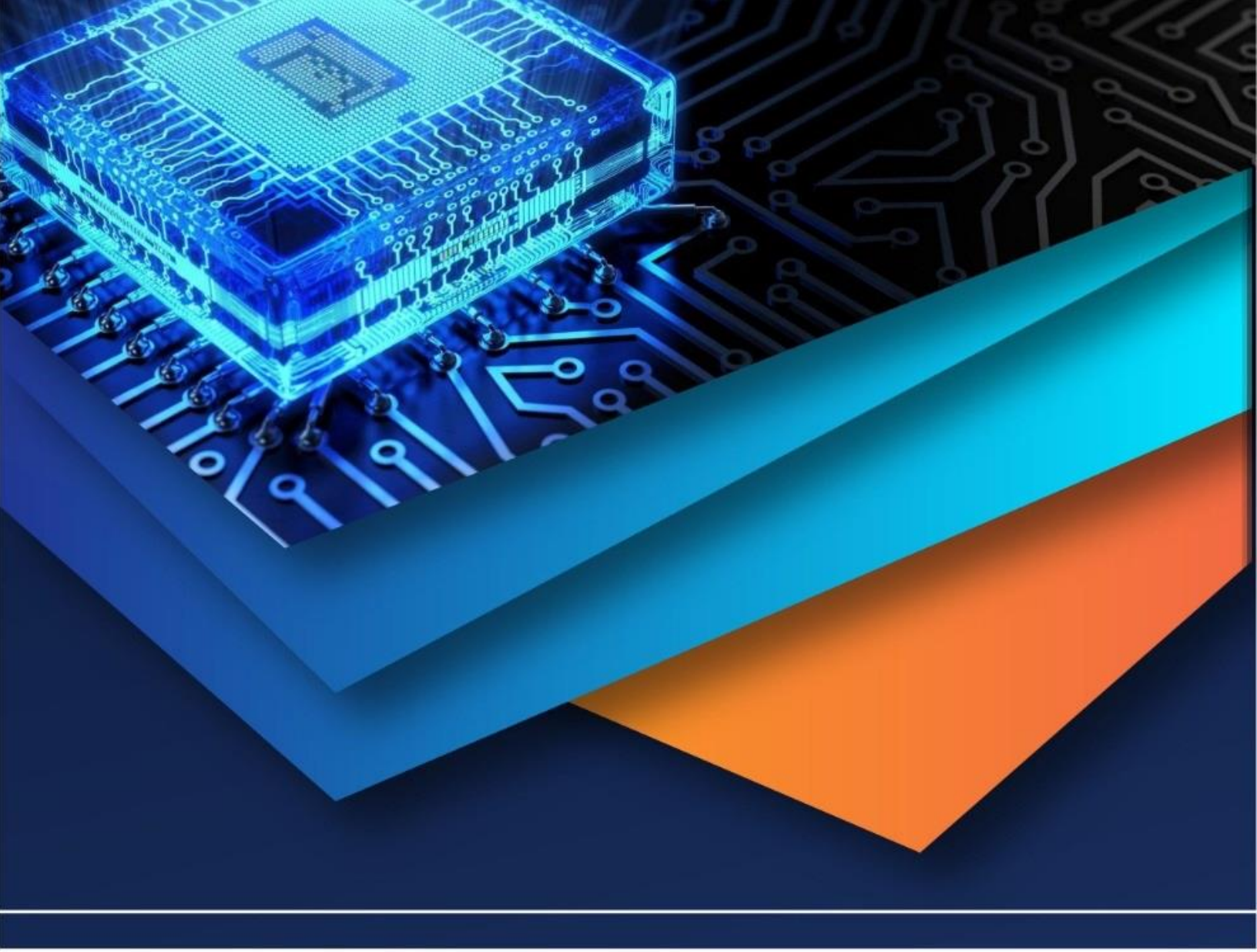

10.22214/IJRASET

45.98

IMPACT FACTOR: 7.129

IMPACT FACTOR: 7.429

INTERNATIONAL JOURNAL FOR RESEARCH

IN APPLIED SCIENCE & ENGINEERING TECHNOLOGY